Bone ingrowth in a shoulder prosthesis

E.M.van Aken
1107895
emvanaken@hotmail.com

Delft, 2006-2007

Contents

Chapter 1

Introduction

As a result of osteoporosis, osteoarthritis, rheumatoid arthritis or severe trauma from a shoulder fracture, it is possible that the shoulder joint dysfunctions. The cartilage is thinner than it is supposed to be or the bones are too weak. As a result the bones rub together causing pain, swelling and/or loss of motion of the joint.
To improve the movement of the joint and to relief the pain, a prosthesis to replace the glenoid of the shoulder joint is an option.

The shoulder is a ball-and socket joint, which means that the end of one bone has a ball-like surface which is surrounded by a concave socket (the end of the other bone). The range of motion of the joint is determined by the rate of coverage of the ball by the socket, see figure 1.1.

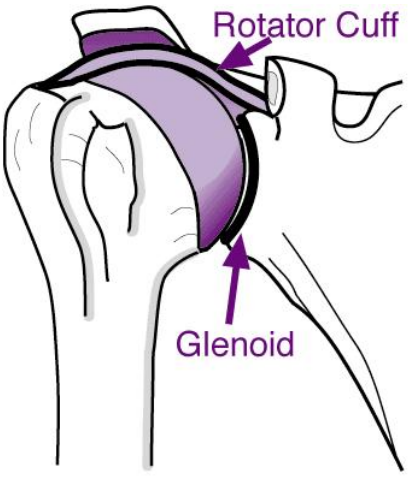

Figure 1.1: The shoulder joint is a ball-and-socket joint [1]

The glenoid is the cavity of the scapula (shoulder blade) in which the upper arm fits.
The prosthesis, often made of stainless steal combined with polyethylene, re-

places this glenoid cavity and is made of porous material at the bone side. This way bone can grow into the prosthesis, which leads to a fusion of bone and prosthesis.
However, it is possible that no bone ingrowth will occur at all, if the mechanical stress is too low. For this reason it is important to know what the stress distribution should be and what material is best to be used for the prosthesis, to make sure the bone ingrowth is optimal. The model to simulate the bone ingrowth consists of two parts: one part relating to the biophysical stimuli and the other part relating to the tissue differentiation. In this report the tissue differentiation will be discussed by using two different models. Chapter 2 explains the cell differentiation process, which is similar to the process of secondary healing of a bone fracture.
Several models describing this process will be discussed. For two models the differential equations will be given and boundary conditions will be derived.
The models can be solved using numerical methods. These methods and the discretisation of the differential equations of the model of Prendergast will be given in chapter 3. This will be implemented in MATLAB to get a solution.
In chapter 4 the results will be given and also a sensitivity analysis will be shown. In chapter 5 some conclusions will be drawn and the future goals for this project are given in chapter 6.

Chapter 2

Models

The cell differentiation during bone ingrowth in an artificial shoulder is actually the same process as the cell differentiation during a secondary fracture healing. Fracture healing begins as undifferentiated mesenchymal cells migrate from the periosteum and the surroundings (like muscles). They produce initial connective tissue around the fracture side, forming an initial stabilizing callus [Bailon-Plaza, A. and M. C. H Van der Meulen(2001)]. This callus depends on the size of the fracture gap and the mechanical stability.
Healing processes can be divided into two groups: primary healing and secondary healing. Primary healing takes place when the fracture size is very small and stable. The bone fragments get reattached by direct bone remodelling, forming a very small or no callus.
In most cases fractures heal by secondary healing. This happens when the fracture size is relatively big or unstable. Secondary healing can be divided into four stages: Inflammation, callus differentiation, ossification and remodelling, see figure 2.1.

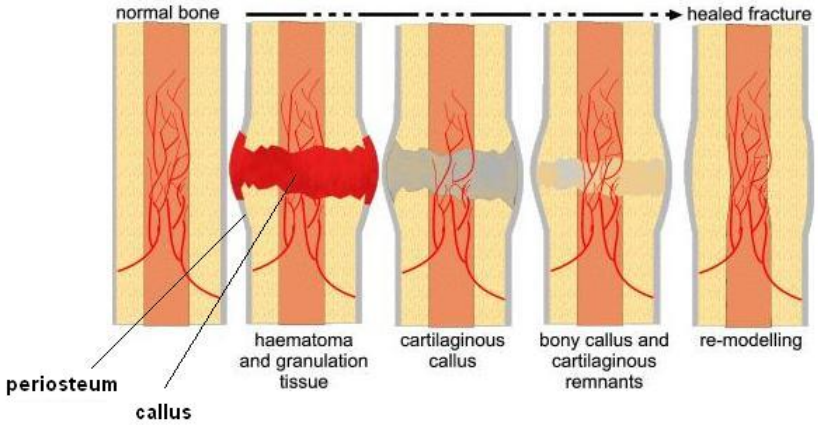

Figure 2.1: The different stages during the process of bone fracture healing [2]

During the inflammation stage blood cells, coming from the ruptured blood vessels, form a fibrin matrix. Mesenchymal cells originate from the broken periosteum and replace the fibrin matrix to form the external callus.
Depending on the mechanical and biological environment the mesenchymal cells differentiate into fibroblast (cells forming fibrous tissue), chondrocytes (cartilage-forming cells) or osteoblast (bone-forming cells). During callus differentiation mesenchymal cells along the bone side differentiate into osteoblasts, which begin to actively synthesize intra-membranous woven bone. In the interior of the callus mesenchymal cells differentiate into chondrocytes, while mesenchymal cells that reach the fracture gap will differentiate into fibroblasts. During healing the intra-membranous ossification front advances towards the center of the callus and the chondrous callus grows due mesenchymal cell differentiation into chondrocytes and chondrocytic proliferation. As time goes on ossification of the cartilage callus starts, called endochondral ossification.
During endochondral ossification chondrocytes undergo apoptosis and will be replaced with osteoblasts. This process continues until all the cartilage is replaced with bone and the fracture gap is closed.
The last stage of bone remodelling starts when the fracture gap is ossified and ends with the restoration of the original form of the bone. This last stage has not been studies in the models presented here.

2.1 Model of Prendergast

The first model to be dealt with is the model of Prendergast. This models describes the behavior of the mesenchymal cells, the fibroblasts, the chondrocytes and the osteoblasts and also the matrix production caused by these various cell types[Andreykiv, A (2006)].
Since it is assumed that the mesenchymal cells and the fibroblasts migrate through the callus they are modelled by means of a diffusion-reaction equation. The chondrocytes and the osteoblasts are assumed not to migrate, so their equations do not contain diffusion terms.
For all these cell types there is one term that describes the proliferation of the cell type and one or more terms to describe the differentiation of the cells (see figure 2.2). For example the mesenchymal cells can differentiate into fibroblasts, chondrocytes or osteoblasts, so the equations for the mesenchymal cells contains three differentiation terms. The matrix densities are influenced by the production and resorption rates of the various tissues and the cellular densities of the corresponding tissue. The resorption rates are chosen to be equal to the production rates.

The following symbols will be used:
c_i represent the cellular densities, $c_{tot} = c_m + c_c + c_b + c_f$
m_i represent the matrix densities, $m_{tot} = m_c + m_b + m_f$
D_i are the diffusion coefficients (depending on m), for $i = m, f$
P_i are the proliferations rates
F_i are the differentiation rates
Q_i the production rates of the tissue(matrix)
D_i are the tissue resorption rates (equal to Q), for $i = c, b$

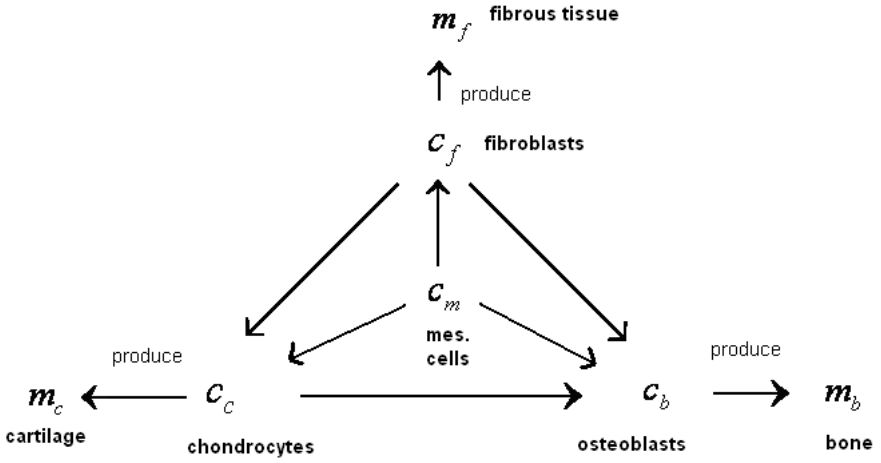

Figure 2.2: Mesenchymal cells can differentiate into fibroblasts, chondrocytes or osteoblasts. Fibroblasts can differentiate into chondrocytes and osteoblasts. Chondrocytes can differentiate into osteoblasts.

Initially the callus is only filled with granulation tissue and all the cell concentrations are zero. Thus the initial conditions are given by

$$c_i(\underline{x}, 0) = m_i(\underline{x}, 0) = 0.$$

Mesenchymal cells originate from the periosteum layer and the bone marrow, hence the mesenchymal cell density at those areas is kept constant at the highest saturation level, thus

$$c_m|_{periosteum} = c_{max}, \forall t.$$

The change in the cellular densities can be described by the following partial differential equations:

$$\begin{aligned} \frac{\partial c_m}{\partial t} &= D_m \nabla^2 c_m + P_m(1 - c_{tot})c_m - F_f(1 - c_f)c_m - F_c(1 - c_c)c_m \\ &\quad -F_b(1 - c_b)c_m. \end{aligned} \tag{2.1}$$

$$\begin{aligned} \frac{\partial c_f}{\partial t} &= D_f \nabla^2 c_f + P_f(1 - c_{tot})c_f + F_f(1 - c_f)c_m - F_c(1 - c_c)c_f \\ &\quad -F_b(1 - c_b)c_f. \end{aligned} \tag{2.2}$$

$$\frac{\partial c_c}{\partial t} = P_c(1 - c_{tot})c_c + F_c(1 - c_c)(c_m + c_f) - F_b(1 - c_b)c_c, \tag{2.3}$$

$$\frac{\partial c_b}{\partial t} = P_b(1 - c_{tot})c_b + F_b(1 - c_b)(c_m + c_f + c_c). \tag{2.4}$$

The first terms on the right hand side of (2.1) and (2.2) represent the diffusion of the mesenchymal cells and the fibroblasts respectively. The second terms represent the proliferation of the cells. The last three terms of (2.1) express the differentiation from mesenchymal cells into fibroblasts, chondrocytes and osteoblasts. These last terms will come back in the equations for the other cell types.
The third term of (2.2) represents the cells which differentiated from mesenchymal cells into fibroblasts. The fourth and fifth term of (2.2) represent the differentiation of fibroblasts into chondrocytes and osteoblasts.
The equations for cartilage cellular density (2.3) and bone cellular density (2.4) only contain terms for proliferation and differentiation.

For the change in the matrix densities the following differential equations are derived:

$$\frac{\partial m_f}{\partial t} = Q_f(1 - m_{tot})c_f - (D_b c_b + D_c c_c)m_f m_{tot}, \tag{2.5}$$

$$\frac{\partial m_c}{\partial t} = Q_c(1 - m_b - m_c)c_c - D_b c_b m_c m_{tot}, \tag{2.6}$$

$$\frac{\partial m_b}{\partial t} = Q_b(1 - m_b)c_b. \tag{2.7}$$

The first terms on the right hand side of (2.5), (2.6) and (2.7) express the production of the tissue. The second terms on the right hand side of (2.5) and (2.6) represent the resorption of the tissue.

All equations and parameters are non-dimensionalized.
Cell differentiation, proliferation and tissue production are regulated by tissue shear strain and interstitial fluid velocity, so P, F, Q depend on S. The following equation holds for S:

$$S = \frac{\gamma}{a} + \frac{\nu}{b}, \tag{2.8}$$

where γ represents the maximum shear strain and ν the fluid/solid velocity.

2.2 Model due to Bailon-Plaza

Another model to investigate is the model by Bailon-Plaza [Bailon-Plaza, A. and M. C. H Van der Meulen(2001)]. This model leaves out the fibroblasts and the fibrous tissue and has extra equations for the growth factors of bone and cartilage .
Growth factors are proteins that are involved in cell differentiation and growth [3]. So they influence the differentiation rates from mesenchymal cells into either osteoblasts or chondrocytes and the endochondral replacement of the chondrocytes. Unlike the previous model, where the growth factors themselves are not modelled, here their behavior is described by means of a

convection-diffusion-reaction equation. So they are assumed to migrate and they are depending on their corresponding cellular densities and the growth factor production rates.
For the mesenchymal cells, chondrocytes and osteoblasts and the bone and cartilage matrix densities the same sort of equations are chosen as in the previous model.
The non-dimensionalized model looks as follows:
The equations for the change in mesenchymal, cartilage and bone cell densities are

$$\frac{\partial c_m}{\partial t} = \nabla \cdot (D\nabla c_m - C c_m \nabla m) + A_m c_m (1 - \alpha_m c_m) - F_1 c_m - F_2 c_m, \quad (2.9)$$

$$\frac{\partial c_c}{\partial t} = A_c c_c (1 - \alpha_c c_c) + F_2 c_m - F_3 c_c, \quad (2.10)$$

$$\frac{\partial c_b}{\partial t} = A_b c_b (1 - \alpha_b c_b) + F_1 c_m + F_3 c_c - d_b c_b, \quad (2.11)$$

where D and C represent the haptotactic and haptokinetic cell migration speeds. The proliferation rates are denoted by A_m, A_c and A_b, F_1 is the mesenchymal differentiation into osteoblasts, F_2 the mesenchymal differentiation into chondrocytes and F_3 the endochondral replacement of chondrocytes. The symbol d_b stands for osteoblasts removal and the α_i's result from non-dimensionalizing the equations.
The changes in cartilage and bone matrix densities are modelled in the following way:

$$\frac{\partial m_c}{\partial t} = P_{cs}(1 - \kappa_c m_c)(c_m + c_c) - Q_{cd} m_c c_b, \quad (2.12)$$

$$\frac{\partial m_b}{\partial t} = P_{bs}(1 - \kappa_b m_b) c_b, \quad (2.13)$$

where P_{cs} and P_{bs} represent constants of cartilage and bone matrix production and Q_{cd} is a constant of matrix degradation.
The growth factor concentrations g_c and g_b are modelled in the following way:

$$\frac{\partial g_c}{\partial t} = \frac{\partial}{\partial x}(D_{gc}\frac{\partial g_c}{\partial x}) + E_{gc} c_c - d_{gc} g_c, \quad (2.14)$$

$$\frac{\partial g_b}{\partial t} = \frac{\partial}{\partial x}(D_{gb}\frac{\partial g_b}{\partial x}) + E_{gb} c_b - d_{gb} g_b, \quad (2.15)$$

where D_{gc} and D_{gb} are diffusion coefficients, E_{gc} and E_{gb} are functions relating growth factor production to growth factor concentration, and d_{gc} and d_{gb} are constants of decay.
The initial and boundary conditions for the cellular densities and the matrix densities are given by

$$c_m|_{periosteum} = c_{max}, \qquad \left.\frac{\partial c_m}{\partial x}\right|_{other\ boundaries} = 0, \qquad \forall t$$

$$c_m(\underline{x},0)=0, \quad c_c(\underline{x},0)=0, \quad c_b(\underline{x},0)=0.$$

$$m_b(\underline{x},0)=0, \qquad m_c(\underline{x},0)=0.1.$$

The initial and boundary conditions for the growth factors are given by

$$g_i(\underline{x},0)=0,$$

where $i=c,b$.
For $t \leq t_K$

$$g_c|_{fracture\ gap}=20, \qquad g_b|_{along\ bone}=20, \qquad \left.\frac{\partial g_i}{\partial x}\right|_{other\ boundaries}=0.$$

For $t > t_K$

$$\left.\frac{\partial g_i}{\partial x}\right|_{all\ boundaries}=0,$$

where $i=c,b$.
t_K is the time whereafter no growth factors will originate anymore from the fracture gap and along the bone respectively.
At last the functions are defined by:

$$D=\frac{D_h}{(K_h^2+m^2)}m, \tag{2.16}$$

$$C=\frac{C_k}{(K_k+m)^2}, \tag{2.17}$$

$$A_m=\frac{A_{m0}}{(K_m^2+m^2)}m, \tag{2.18}$$

$$A_c=\frac{A_{c0}}{(K_c^2+m^2)}m, \tag{2.19}$$

$$A_b=\frac{A_{b0}}{(K_b^2+m^2)}m, \tag{2.20}$$

$$F_1=\frac{Y_1}{(H_1+g_b)}g_b, \tag{2.21}$$

$$F_2=\frac{Y_2}{(H_2+g_c)}g_c, \tag{2.22}$$

$$F_3=(\frac{m_c^6}{B_{ec}^6+m_c^6})(\frac{Y_3}{H_3+g_b})g_b, \tag{2.23}$$

$$E_{gc} = (\frac{G_{gc}g_c}{H_{gc} + g_c})(\frac{m}{K_{gc}^3 + m^3}), \tag{2.24}$$

$$E_{gb} = \frac{G_{gb}g_b}{(H_{gb} + g_b)}, \tag{2.25}$$

where D_h, K_h,C_k, K_k, A_{m0}, K_m, A_{c0}, K_c, A_{b0}, K_b, Y_1, H_1, Y_2, H_2, Y_3, H_3, B_{ec}, G_{gc}, H_{gc}, K_{gc}, G_{gb} and H_{gb} are constants.
The functions and constants are not regulated by mechanical stimuli.

2.3 Other Models

2.3.1 Model of Ament and Hofer

Another, totally different, model for fracture healing is the model due to Ament and Hofer [Ament, Ch. and E. P. Hofer (2000)]. It is an algorithm which also consist of a mechanical stimuli part and a tissue differentiation part, only here both should be determined during every time step. The three types of tissues that are involved here: cartilage, bone and fibrous connective tissue. The latter contains also granulation tissue in this model. It is assumed that each element is completely composed by these three types of tissue.

For every time step look for each element at the tissue composition and the dominating part of it, to figure out if it is fibrous tissue, cartilage or bone. The strain energy density can be determined using the modulus of elasticity and the Poisson's ratio. The tissue differentiation is determined by the spatial change of the bone matrix density. This is called the osteogenic factor. This will be calculated for every element.
Finally, when both the strain energy density and the osteogenic factor are determined, one can calculate the tissue differentiation rates per element, which leads to the new tissue composition.

2.3.2 Model of Adam

The model due to Adam[Adam, J. A. (1999)] examines the conditions under which wound healing will occur.

A thin layer of bone at the wound edges manufactures growth factors. In 1D these layers lie at $-L/2 \leq x \leq -L/2 - \delta$ and $L/2 \leq x \leq L/2 + \delta$. The wound width lies at $-L/2 \leq x \leq L/2$.
Since this problem is symmetric from now on only the domain $[0, \infty)$ will be considered. The goal is to find a value for δ, so healing will occur.
The fundamental equation for the growth factor concentration is described by

$$\frac{\partial C}{\partial t} = D\frac{\partial^2 C}{\partial x^2} - \lambda C + PS(x), \tag{2.26}$$

where D is the diffusion coefficient of the growth factor, λ the decay of the growth factor and P the production rate of the growth factor. These are all

constants. $S(x)$ is the source term, describing the distribution of the growth factors, which is chosen to be uniform (so $S(x) = 1$ at $L/2 \leq x \leq L/2 + \delta$ and $S(x) = 0$ elsewhere).
It is assumed that the distribution is independent of time, so $\frac{\partial C}{\partial t} = 0$. Furthermore the assumption has been made that the growth factors regulate the growth of bone. Also it is presumed that there are no mechanical constraints, so the bone is free to grow into the wound.

Now the equation can be written as

$$\frac{d^2C}{dx^2} - \frac{\lambda}{D}C = -\frac{P}{D}, \qquad \frac{L}{2} \leq x \leq \frac{L}{2} + \delta \tag{2.27}$$

and

$$\frac{d^2C}{dx^2} - \frac{\lambda}{D}C = 0, \tag{2.28}$$

elsewhere.
Two models are investigated. In the first model it is assumed there is no tissue in the wound interior $-L/2 \leq x \leq L/2$, in the second model it is assumed there is still some tissue in the wound interior.

The boundary conditions for model 1 are given by
(i) $C(x)$, $\frac{dC}{dx}$ are continuous at $x = L/2 + \delta$
(ii)$\lim_{x\to\infty} C(x) = 0$
(iii)$\frac{dC}{dx} = 0$ at $x = L/2$

and the boundary condition for model 2 are given by
(i) $C(x)$, $\frac{dC}{dx}$ are continuous at $x = L/2$ and $x = L/2 + \delta$
(ii)$\lim_{x\to\infty} C(x) = 0$
(iii)$\frac{dC}{dx} = 0$ at $x = 0$

Solving these models values for δ are obtained for which healing will occur.

Chapter 3

Numerical Methods

To solve these differential equations numerical methods will be used. First a discretisation in space should be performed and then a discretisation in time. There are several methods to this purpose.

3.1 Discretisation in space

For the first derivative in space a very commonly used method is the *central-scheme*. The equidistant grid is divided in N_x parts. The scheme looks as follows:

$$\frac{\partial u}{\partial x} \simeq \frac{u_{j+1} - u_{j-1}}{2h}, \tag{3.1}$$

where j are the data points and $h = 1/N_x$ is the spatial step size. For the second derivative the *three-point-method* is often used:

$$\frac{\partial^2 u}{\partial x^2} \simeq \frac{u_{j+1} - 2u_j + u_{j-1}}{h^2}. \tag{3.2}$$

Both schemes are of order h^2.

Another possible scheme is *upwind discretisation*:

$$\frac{\partial u}{\partial x} \simeq \frac{u_j - u_{j-1}}{h}. \tag{3.3}$$

This method is of order h.

Another method also very often used is the *Finite Volume method*. Very briefly this method works as follows:
(1) The domain is subdivided segments,also called control volumes, with length h_j, $j = 1, ..., N$.
(2) In a vertex-centered grid the nodes j are distributed over the domain and also at the boundaries nodes are put. The boundaries of the control volumes are centered between the nodes.
(3) The equation will be integrated over the control volumes to obtain the scheme.
For further details see [Wesseling, P. (2002)].

3.2 Discretisation in time

For discretisation in time the most commonly used scheme is the *backward Euler scheme*. Consider the equation

$$\frac{\partial u}{\partial t} = f(t, u), \tag{3.4}$$

where f is a function. Then the backward Euler scheme leads to

$$\frac{u^{n+1} - u^n}{\tau} = f(t^{n+1}, u^{n+1}), \tag{3.5}$$

where τ is the step size in time. This is an implicit method.
Also the ω-scheme can be used, which is a combination of the forward and the backward Euler scheme($0 \leq \omega \leq 1$):

$$\frac{u^{n+1} - u^n}{\tau} = (1 - \omega) f(t^n, u^n) + \omega f(t^{n+1}, u^{n+1}) \tag{3.6}$$

Another possible method is the Runge-Kutta-4 method [Burden, R. L. and J. D. Faires (2001)]. This is an explicit method and works as follows:
Calculate

$$K_1 = \tau f(t^n, u^n)$$

$$K_2 = \tau f(t^n + \frac{\tau}{2}, u^n + \frac{K_1}{2})$$

$$K_3 = \tau f(t^n + \frac{\tau}{2}, u^n + \frac{K_2}{2})$$

$$K_4 = \tau f(t^n + \tau, u^n + K_3)$$

and set

$$u^{n+1} = u^n + \frac{1}{6}(K_1 + 2K_2 + 2K_3 + K_4) \tag{3.7}$$

3.3 Application to the model of Prendergast

For the 1D discretisation of the model of Prendergast the central scheme and the three-point method are used for discretisation in space. An equidistant grid is used. The backward Euler method is used for discretisation in time.

3.3.1 Mesenchymal cellular density

For the first equation, the one for the mesenchymal cellular density, the equation in 1D is:

$$\begin{aligned}\frac{\partial c_m}{\partial t} &= D_m\frac{\partial^2 c_m}{\partial x^2} + P_m(1-c_{tot})c_m - F_f(1-c_f)c_m \\ &\quad -F_c(1-c_c)c_m - F_b(1-c_b)c_m.\end{aligned} \tag{3.8}$$

After discretisation in space it follows for an interior point $j = 2, .., N_x - 1$

$$\begin{aligned}\frac{\partial c_{m(j)}}{\partial t} &= D_{m(j)}\frac{c_{m(j-1)} - 2c_{m(j)} + c_{m(j+1)}}{h^2} + P_{m(j)}(1-c_{tot(j)})c_{m(j)} \\ &\quad -F_f(1-c_{f(j)})c_{m(j)} - F_c(1-c_{c(j)})c_{m(j)} - F_b(1-c_{b(j)})c_{m(j)}.\end{aligned} \tag{3.9}$$

For $j = 1$ holds:

$$\begin{aligned}\frac{\partial c_{m(1)}}{\partial t} &= D_{m(1)}\frac{c_{max} - 2c_{m(1)} + c_{m(2)}}{h^2} + P_{m(1)}(1-c_{tot(1)})c_{m(1)} \\ &\quad -F_f(1-c_{f(1)})c_{m(1)} - F_c(1-c_{c(1)})c_{m(1)} - F_b(1-c_{b(1)})c_{m(1)},\end{aligned} \tag{3.10}$$

and for $j = N_x$, using a virtual point and the Neumann boundary condition:

$$\begin{aligned}\frac{\partial c_{m(N_x)}}{\partial t} &= D_{m(N_x)}\frac{2c_{m(N_x-1)} - 2c_{m(N_x)}}{h^2} \\ &\quad +P_{m(N_x)}(1-c_{tot(N_x)})c_{m(N_x)} \\ &\quad -F_f(1-c_{f(N_x)})c_{m(N_x)} - F_c(1-c_{c(N_x)})c_{m(N_x)} \\ &\quad -F_b(1-c_{b(N_x)})c_{m(N_x)}.\end{aligned} \tag{3.11}$$

So at the end it becomes a time-dependent vector-differential equation:

$$\frac{\partial \underline{c}_m}{\partial t} = Z_{cm}\underline{c}_m + \underline{f}_m. \tag{3.12}$$

Here Z_{cm} is an $N_x \times N_x$ tridiagonal matrix, represented by

$$\begin{bmatrix} B_1 & A_1 & .. & .. & .. & .. \\ A_2 & B_2 & A_2 & .. & .. & .. \\ .. & A_3 & B_3 & \ddots & .. & .. \\ .. & .. & \ddots & \ddots & \ddots & .. \\ .. & .. & . & A_{N_x-1} & B_{N_x-1} & A_{N_x-1} \\ .. & .. & .. & .. & 2A_{N_x} & B_{N_x} \end{bmatrix},$$

where

$$A_i = \frac{D_{m(i)}}{h^2}$$

and

$$B_i = \frac{-2D_{m(i)}}{h^2} + P_{m(i)}(1-c_{tot(i)}) - F_f(1-c_{f(i)}) - F_c(1-c_{c(i)}) - F_b(1-c_{b(i)})$$

Further the following functions are defined:

$$P_m = P_{m0}(1 - m_c - m_b), \qquad D_m = D_{m0}(1 - m_c - m_b)$$

and $\underline{c}_m$ and $\underline{f}_m$ are represented by:

$$\underline{c}_m = \begin{bmatrix} c_{m(1)} \\ c_{m(2)} \\ .. \\ .. \\ c_{m(N_x-1)} \\ c_{m(N_x)} \end{bmatrix}$$

and

$$\underline{f}_m = \begin{bmatrix} A_{(1)}c_{max} \\ 0 \\ .. \\ .. \\ .. \\ 0 \end{bmatrix},$$

where the first entry of the vector f_m follows from the Dirichlet-boundary condition given on the periosteum.

Now discretisation in time can be applied. The values for c_m will be taken implicit and the other variables will be taken explicit. However, the equation contains a non-linear term c_m^2, so a problem arises. This will be solved by using Picard linearization, which means $(c_m^{n+1})^2$ will be replaced by $c_m^n c_m^{n+1}$. So the discretisation in time becomes semi-implicit method. This will also be done for other non-linear terms in this report. It follows(for simplicity the underlining is left behind):

$$\frac{c_m^{n+1} - c_m^n}{\tau} = Z_{cm}^n c_m^{n+1} c_m^{n+1} + f_m^n. \tag{3.13}$$

Collecting terms gives:

$$c_m^{n+1} = c_m^n + \tau(Z_{cm}^n c_m^{n+1} + f_m^n) \tag{3.14}$$

and finally

$$(I - \tau(Z_{cm}^n - P_m^n c_m^n))c_m^{n+1} = c_m^n + \tau f_m^n. \tag{3.15}$$

3.3.2 Fibrous cellular density

The discretisation of the differential equation for the fibrous cellular density follows the same procedure as for the mesenchymal cellular density. So the equation

$$\begin{aligned} \frac{\partial c_f}{\partial t} &= D_f \frac{\partial^2 c_f}{\partial x^2} + P_f(1 - c_{tot})c_f + F_f(1 - c_f)c_m \\ &\quad -F_c(1 - c_c)c_f - F_b(1 - c_b)c_f \end{aligned} \tag{3.16}$$

becomes

$$\begin{aligned}\frac{\partial c_{f(j)}}{\partial t} &= D_{f(j)}\frac{c_{f(j-1)}-2c_{f(j)}+c_{f(j+1)}}{h^2}+P_{f(j)}(1-c_{tot(j)})c_{f(j)} \\ &+F_f(1-c_{f(j)})c_{m(j)}-F_c(1-c_{c(j)})c_{f(j)}-F_b(1-c_{b(j)})c_{f(j)},\end{aligned} \tag{3.17}$$

for $j = 2, ..., N_x - 1$.

For $j = 0$, using a virtual point and the fact that it is Neumann boundary, it holds:

$$\begin{aligned}\frac{\partial c_{f(0)}}{\partial t} &= D_{f(0)}\frac{-2c_{f(0)}+2c_{f(j+1)}}{h^2}+P_{f(0)}(1-c_{tot(0)})c_{f(0)} \\ &+F_f(1-c_{f(0)})c_{m(0)}-F_c(1-c_{c(0)})c_{f(0)}-F_b(1-c_{b(0)})c_{f(0)},\end{aligned} \tag{3.18}$$

and for $j = N_x$, which is also a Neumann boundary:

$$\begin{aligned}\frac{\partial c_{f(N_x)}}{\partial t} &= D_{f(N_x)}\frac{2c_{f(N_x-1)}-2c_{f(N_x)}}{h^2}+P_{f(N_x)}(1-c_{tot(N_x)})c_{f(N_x)} \\ &+F_f(1-c_{f(N_x)})c_{m(N_x)}-F_c(1-c_{c(N_x)})c_{f(N_x)}-F_b(1-c_{b(N_x)})c_{f(N_x)},\end{aligned} \tag{3.19}$$

So at the end a time-dependent vector-differential equation is obtained:

$$\frac{\partial \underline{c}_f}{\partial t} = Z_{cf}\underline{c}_f + \underline{f}_f, \tag{3.20}$$

where Z_{cf} is the tridiagonal $(N_x + 1) \times (N_x + 1)$ matrix

$$\begin{bmatrix} B_0 & 2A_0 & .. & .. & .. & .. \\ A_1 & B_1 & A_1 & .. & .. & .. \\ .. & A_2 & B_2 & \ddots & .. & .. \\ .. & .. & \ddots & \ddots & \ddots & .. \\ .. & .. & . & A_{N_x-1} & B_{N_x-1} & A_{N_x-1} \\ .. & .. & .. & .. & 2A_{N_x} & B_{N_x} \end{bmatrix},$$

and

$$A_i = \frac{D_{f(i)}}{h^2}$$

and

$$B_i = \frac{-2D_{f(i)}}{h^2} + P_{f(i)}(1-c_{tot(i)}) + F_f(1-c_{f(i)}) - F_c(1-c_{c(i)}) - F_b(1-c_{b(i)})$$

Further

$$P_f = P_{f0}(1-m_c-m_b), \qquad D_f = D_{f0}(1-m_c-m_b), \qquad \underline{f}_f = F_f c_m$$

and $\underline{c}_f$ is represented by:

$$\underline{c}_f = \begin{bmatrix} c_{f(0)} \\ c_{f(1)} \\ .. \\ .. \\ c_{f(N_x-1)} \\ c_{f(N_x)} \end{bmatrix}.$$

For the discretisation in time again a semi-implicit method is used, because of the non-linear term in the equation. It follows (again for simplicity the underlining is left behind):

$$\frac{c_f^{n+1} - c_f^n}{\tau} = Z_{cf}^n c_f^{n+1} + f_f^n. \tag{3.21}$$

Collecting terms gives:

$$c_f^{n+1} = c_f^n + \tau(Z_{cf}^n c_f^{n+1} + f_f^n), \tag{3.22}$$

and finally

$$(I - \tau(Z_{cf}^n - P_f^n c_f^n))c_f^{n+1} = c_f^n + \tau f_f^n. \tag{3.23}$$

3.3.3 Cartilage cellular density

For the differential equation for chondrocytes no discretisation in space is needed, only a discretisation in time.
First collect terms:

$$\begin{aligned} \frac{\partial c_c}{\partial t} &= P_c(1 - c_{tot})c_c + F_c(c_m + c_f) - F_c(c_m + c_f)c_c \\ &\quad -F_b(1 - c_b)c_c \\ &= (P_c(1 - c_f - c_m - c_b) - F_c(c_m + c_f) - F_b(1 - c_b))c_c \\ &\quad +F_c(c_m + c_f) \\ &= Z_{cc}c_c + f_c, \end{aligned} \tag{3.24}$$

where the rows of Z_{cc} are represented by

$$Z_{cc} = \begin{bmatrix} 0 & P_c(1 - c_{tot}) - F_c(c_m + c_f) - F_b(1 - c_b) & 0 \end{bmatrix}$$

and

$$P_c = P_{c0}(1 - m_c - m_b), \qquad f_c = F_c(c_m + c_f). \tag{3.25}$$

Now discretisation in time can be applied. It follows:

$$(I - \tau Z_{cc}^n)c_c^{n+1} = c_c^n + \tau f_c^n. \tag{3.26}$$

3.3.4 Bone cellular density

Also the differential equation for osteoblasts only needs time-discretisation, because there are no derivatives in space.

$$\begin{aligned} \frac{\partial c_b}{\partial t} &= P_b(1 - c_{tot}c_b + F_b(c_m + c_f + c_c) \\ &\quad -F_b(c_m + c_f + c_c)c_b \\ &= (P_b(1 - c_{tot}) - F_b(c_m + c_f + c_c))c_b \\ &\quad +F_c(c_m + c_f + c_c) \\ &= Z_{cb}c_b + f_b, \end{aligned} \tag{3.27}$$

with

$$Z_{cb} = \left[\begin{array}{ccc} 0 & P_b(1-c_{tot}) - F_b(c_m + c_f + c_c) & 0 \end{array} \right],$$

$$P_b = P_{b0}(1 - m_c - m_b), \qquad f_b = F_b(c_m + c_f + c_c). \tag{3.28}$$

Applying time-discretisation:

$$(I - \tau Z_{cb}^n) c_b^{n+1} = c_b^n + \tau f_b^n. \tag{3.29}$$

3.3.5 Discretisation fibrous matrix density

For the three matrix densities the same holds as for the chondrocyte and osteoblast densities: Only discretisation in time is needed. For fibrous matrix tissue it follows:

$$\begin{aligned} \frac{\partial m_f}{\partial t} &= Q_f(1 - m_{tot})c_f - (D_b c_b + D_c c_c) m_f (m_f + m_c + m_b) \qquad (3.30) \\ &= Q_f(1 - (m_c + m_b))c_f - Q_f c_f m_f - (D_b c_b + D_c c_c)(m_c + m_b) m_f \\ &\quad -(D_b c_b + D_c c_c) m_f^2 \\ &= Z_{mf} m_f - (D_b c_b + D_c c_c) m_f^2 + f_{mf}, \end{aligned}$$

where

$$Z_{mf} = \left[\begin{array}{ccc} 0 & -Q_f c_f - (D_b c_b + D_c c_c)(m_c + m_b) & 0 \end{array} \right]$$

and

$$f_{mf} = Q_f(1 - (m_c + m_b))c_f. \tag{3.31}$$

Applying time-discretisation:

$$\frac{m_f^{n+1} - m_f^n}{\tau} = f_{mf}^n + Z_{mf}^n m_f^{n+1} - (D_b c_b + D_c c_c) m_f^n m_f^{n+1} \tag{3.32}$$

gives

$$(I - \tau(Z_{mf}^n - (D_b c_b + D_c c_c) m_f^n)) m_f^{n+1} = m_f^n + \tau f_{mf}^n. \tag{3.33}$$

3.3.6 Cartilage matrix density

For cartilage matrix the discretisation is as follows:

$$\begin{aligned} \frac{\partial m_c}{\partial t} &= Q_c(1 - m_c - m_b)c_c - D_b c_b m_c (m_f + m_c + m_b) \qquad (3.34) \\ &= Q_c(1 - m_b)c_c - Q_c c_c m_c - D_b c_b (m_f + m_b) m_c - D_b c_b m_c^2 \\ &= Z_{mc} m_c - D_b c_b m_c^2 + f_{mc}, \end{aligned}$$

where

$$Z_{mf} = \left[\begin{array}{ccc} 0 & -Q_c c_c - D_b c_b (m_f + m_b) & 0 \end{array} \right]$$

and

$$f_{mc} = Q_c(1 - m_b)c_c. \tag{3.35}$$

Applying time-discretisation:

$$\frac{m_c^{n+1} - m_c^n}{\tau} = f_{mc}^n + Z_{mc}^n m_c^{n+1} - D_b c_b m_c^n m_c^{n+1} \tag{3.36}$$

gives

$$(I - \tau(Z_{mc}^n - D_b c_b m_c^n)) m_c^{n+1} = m_c^n + \tau f_{mc}^n \tag{3.37}$$

3.3.7 Bone matrix density

Finally, for bone matrix tissue, discretisation is done in the same way as above:

$$\frac{\partial m_b}{\partial t} = Q_b c_b - Q_b c_b m_b \tag{3.38}$$

$$\frac{m_b^{n+1} - m_b^n}{\tau} = Q_b c_b^n - Q_b c_b^n m_b^{n+1} \tag{3.39}$$

$$(I + \tau Q_b c_b^n) m_b^{n+1} = m_b^n + \tau Q_b c_b^n \tag{3.40}$$

3.4 Application to the model of Bailon-Plaza

3.4.1 Mesenchymal cellular density

The 1D equation for the mesenchymal cellular density is represented by

$$\frac{\partial c_m}{\partial t} = \frac{\partial}{\partial x}\left(D\frac{\partial c_m}{\partial x} - C c_m \frac{\partial m}{\partial x}\right) + A_m c_m (1 - \alpha_m c_m) - F_1 c_m - F_2 c_m. \tag{3.41}$$

3.4.2 Discretisation in space

For this model the Finite Volume Method will be used for discretisation in space. This because of the derivative of m in the convection term. An equidistant vertex-centered grid will be used.
For a point in the interior this method leads to the following:

$$\begin{aligned}\int_{x_{j-1/2}}^{x_{j+1/2}} \frac{\partial c_m}{\partial t} dx &= \int_{x_{j-1/2}}^{x_{j+1/2}} \frac{\partial}{\partial x}\left(D\frac{\partial c_m}{\partial x}\right) dx \\ &\quad - \int_{x_{j-1/2}}^{x_{j+1/2}} \frac{\partial}{\partial x}\left(C c_m \frac{\partial m}{\partial x}\right) dx \\ &\quad + \int_{x_{j-1/2}}^{x_{j+1/2}} A_m c_m (1 - \alpha_m c_m) dx - \int_{x_{j-1/2}}^{x_{j+1/2}} (F_1 + F_2) c_m dx.\end{aligned} \tag{3.42}$$

The first two integrals of the right hand side can immediately be determined:

$$\begin{aligned}\int_{x_{j-1/2}}^{x_{j+1/2}} \frac{\partial c_m}{\partial t} dx &= \left[D\frac{\partial c_m}{\partial x}\right]_{x_{j-1/2}}^{x_{j+1/2}} - \left[C c_m \frac{\partial m}{\partial x}\right]_{x_{j-1/2}}^{x_{j+1/2}} \\ &\quad + \int_{x_{j-1/2}}^{x_{j+1/2}} A_m c_m (1 - \alpha_m c_m) dx - \int_{x_{j-1/2}}^{x_{j+1/2}} (F_1 + F_2) c_m dx.\end{aligned} \tag{3.43}$$

Assuming an equidistant grid, this leads to the following equation

$$\begin{aligned}\frac{\partial c_{m(j)}}{\partial t}h &= D_{j+1/2}\frac{c_{m(j+1)}-c_{m(j)}}{h} - D_{j-1/2}\frac{c_{m(j)}-c_{m(j-1)}}{h} \\ &\quad -C_{j+1/2}c_{m(j+1/2)}\frac{m_{j+1}-m_j}{h} + C_{j-1/2}c_{m(j-1/2)}\frac{m_j-m_{j-1}}{h} \\ &\quad +\left(A_{m(j)}c_{m(j)}(1-\alpha_m c_{m(j)}) - (F_{1(j)}+F_{2(j)})c_{m(j)}\right)h\end{aligned} \tag{3.44}$$

and dividing by h

$$\begin{aligned}\frac{\partial c_{m(j)}}{\partial t} &= \frac{1}{h}D_{j+1/2}\frac{c_{m(j+1)}-c_{m(j)}}{h} - \frac{1}{h}D_{j-1/2}\frac{c_{m(j)}-c_{m(j-1)}}{h} \\ &\quad -\frac{1}{h}C_{j+1/2}c_{m(j+1/2)}\frac{m_{j+1}-m_j}{h} + \frac{1}{h}C_{j-1/2}c_{m(j-1/2)}\frac{m_j-m_{j-1}}{h} \\ &\quad +(A_{m(j)}c_{m(j)}(1-\alpha_m c_{m(j)}) - (F_{1(j)}+F_{2(j)})c_{m(j)} \\ &= D_{j+1/2}\frac{c_{m(j+1)}-c_{m(j)}}{h^2} - D_{j-1/2}\frac{c_{m(j)}-c_{m(j-1)}}{h^2} \\ &\quad -C_{j+1/2}\frac{c_{m(j+1)}+c_{m(j)}}{2}\frac{m_{j+1}-m_j}{h^2} \\ &\quad +C_{j-1/2}\frac{c_{m(j)}+c_{m(j-1)}}{2}\frac{m_j-m_{j-1}}{h^2} \\ &\quad +A_{m(j)}c_{m(j)}(1-\alpha_m c_{m(j)}) - (F_{1(j)}+F_{2(j)})c_{m(j)}.\end{aligned} \tag{3.45}$$

At the Dirichlet boundary $x = 0$ there is no need to derive an equation for $c_{m(0)}$ because it is prescribed: $c_{m(0)} = c_{max}$.

At the Neumann boundary $x = L$ the control volume has length $h/2$ and applying the Finite Volume Method leads to:

$$\begin{aligned}\int_{x_{N-1/2}}^{x_N}\frac{\partial c_m}{\partial t}dx &= \int_{x_{N-1/2}}^{x_N}\frac{\partial}{\partial x}\left(D\frac{\partial c_m}{\partial x}\right)dx \\ &\quad -\int_{x_{N-1/2}}^{x_N}\frac{\partial}{\partial x}\left(Cc_m\frac{\partial m}{\partial x}\right)dx \\ &\quad +\int_{x_{N-1/2}}^{x_N}A_m c_m(1-\alpha_m c_m)dx - \int_{x_{N-1/2}}^{x_N}(F_1+F_2)c_m dx.\end{aligned} \tag{3.46}$$

This leads to the following equation

$$\begin{aligned}\frac{\partial c_{m(N_x)}}{\partial t}\left(\frac{h}{2}\right) &= \left[D\frac{\partial c_m}{\partial x}\right]_{x_{N-1/2}}^{x_N} - \left[Cc_m\frac{\partial m}{\partial x}\right]_{x_{N-1/2}}^{x_N} \\ &\quad +\left(A_{m(N_x)}c_{m(N_x)}(1-\alpha_m c_{m(N_x)}) - (F_{1(N_x)}+F_{2(N_x)})c_{m(N_x)}\right)\frac{h}{2}.\end{aligned} \tag{3.47}$$

Dividing by $\frac{h}{2}$ and using the Neumann condition

$$\begin{aligned}\frac{\partial c_{m(N_x)}}{\partial t} &= -\frac{2}{h}D_{(N_x-1/2)}\frac{c_{m(N_x)}-c_{m(N_x-1)}}{h} \\ &\quad +\frac{2}{h}C_{(N_x-1/2)}c_{m(N_x-1/2)}\frac{m_{(N_x)}-m_{(N_x-1)}}{h} \\ &\quad +(A_{m(N_x)}c_{m(N_x)}(1-\alpha_m c_{m(N_x)}) - (F_{1(N_x)}+F_{2(N_x)})c_{m(N_x)}\end{aligned} \tag{3.48}$$

$$
\begin{aligned}
= \quad & -D_{(N_x-1/2)}\frac{c_{m(N_x)}-c_{m(N_x-1)}}{h^2} \\
& +C_{(N_x-1/2)}\frac{c_{m(N_x)}+c_{m(N_x-1)}}{2}\frac{m_{N_x}-m_{N_x-1}}{h^2} \\
& +A_{m(N_x)}c_{m(N_x)}(1-\alpha_m c_{m(N_x)})-(F_{1(N_x)}+F_{2(N_x)})c_{m(N_x)}.
\end{aligned}
$$

With (3.45) and (3.48) a vector differential equation is obtained:

$$\frac{\partial \underline{c}_m}{\partial t} = Z_{cm}\underline{c}_m + \underline{f}_{cm}, \tag{3.49}$$

where the rows $j = 1 : N_x - 1$ of the $N_x \times N_x$ matrix Z_{cm} are represented by

$$\left[\begin{array}{ccc} X_j & Y_j & W_j \end{array}\right],$$

and the row $j = N_x$ by

$$\left[\begin{array}{ccc} 2X_j & 2(Y_j - W_j) & 0 \end{array}\right], \text{ with}$$

$$
\begin{aligned}
X_j &= \frac{D_{j-1/2}}{h^2}+\frac{C_{j-1/2}(m_j-m_{j-1})}{2h^2}, \\
Y_j &= \frac{-D_{j+1/2}}{h^2}-\frac{D_{j-1/2}}{h^2}-\frac{C_{j+1/2}(m_{j+1}-m_j)}{2h^2}+\frac{C_{j-1/2}(m_j-m_{j-1})}{2h^2} \\
&\quad +A_{m(j)}(1-\alpha_m c_{m(j)})-(F_{1(j)}+F_{2(j)}), \\
W_j &= \frac{D_{j+1/2}}{h^2}-\frac{C_{j+1/2}(m_{j+1}-m_j)}{2h^2}.
\end{aligned}
$$

$D_{j+1/2}$ and $C_{j+1/2}$ will be approximated by

$$
\begin{aligned}
D_{j+1/2} &\simeq D(\frac{m_{j+1}+m_j}{2}), \\
C_{j+1/2} &\simeq C(\frac{m_{j+1}+m_j}{2}).
\end{aligned}
$$

The vector $\underline{f}_{cm}$ looks as follows:

$$\underline{f}_{cm} = \left[\begin{array}{c} X_1 c_0 \\ 0 \\ \vdots \\ \vdots \\ 0 \\ 0 \end{array}\right].$$

Discretisation in time

Now discretisation in time will be applied. Again the non-linear term $(c_m^{n+1})^2$ will be approximated by $c_m^{n+1}c_m^n$ and ,using the same semi-implicit scheme as seen before, it follows:

$$\frac{c_m^{n+1}-c_m^n}{\tau} = Z_{cm}^n c_m^{n+1} - \alpha_m A_m c_m^n c_m^{n+1} + f_{cm}^n, \tag{3.50}$$

which leads to

$$(I - \tau Z_{cm}^n + \tau \alpha_m A_m c_m^n) c_m^{n+1} = c_m^n + \tau f_{cm}^n. \tag{3.51}$$

3.4.3 Cartilage cellular density

Only discretising in time is necessary because there is only a derivative with respect to time. With the semi-implicit method it becomes:

$$\frac{\partial c_c}{\partial t} = A_c c_c[1 - \alpha_c c_c] + F_2 c_m - F_3 c_c, \tag{3.52}$$

$$\begin{aligned} \frac{c_c^{n+1} - c_c^n}{\tau} &= A_c c_c^{n+1}(1 - \alpha_c c_c^n) + F_2 c_m^n - F_3 c_c^{n+1} \\ &= (A_c - \alpha_c A_c c_c^n - F_3) c_c^{n+1} + F_2 c_m^n, \end{aligned} \tag{3.53}$$

$$(I - \tau A_c + \tau \alpha_c A_c c_c^n + \tau F_3) c_c^{n+1} = c_c^n + \tau F_2 c_m^n. \tag{3.54}$$

3.4.4 Bone cellular density

Again like with the equation for the chondrocytes, only discretising in time is necessary because there is only a derivative with respect to time. With the semi-implicit method it becomes:

$$\frac{\partial c_b}{\partial t} = A_b c_b[1 - \alpha_b c_b] + F_1 c_m + F_3 c_c - d_b c_b, \tag{3.55}$$

$$\begin{aligned} \frac{c_b^{n+1} - c_b^n}{\tau} &= A_b c_b^{n+1}(1 - \alpha_b c_b^n) + F_1 c_m^n + F_3 c_c^n - d_b c_b^{n+1} \\ &= (A_b - \alpha_b A_b c_b^n - d_b) c_b^{n+1} + F_1 c_m^n + F_3 c_c^n, \end{aligned} \tag{3.56}$$

$$(I - \tau A_b + \tau \alpha_b A_b c_b^n + \tau d_b) c_b^{n+1} = c_b^n + \tau F_1 c_m^n + \tau F_3 c_c^n. \tag{3.57}$$

3.4.5 Cartilage matrix density

Discretising in time using the backward Euler scheme gives:

$$\begin{aligned} \frac{\partial m_c}{\partial t} &= P_{cs}(c_m + c_c) - P_{cs}\kappa_c(c_m + c_c) m_c - Q_{cd} c_b m_c \\ &= (-P_{cs}\kappa_c(c_m + c_c) - Q_{cd} c_b) m_c + P_{cs}(c_m + c_c), \end{aligned} \tag{3.58}$$

$$\frac{m_c^{n+1} - m_c^n}{\tau} = (-P_{cs}\kappa_c(c_m^n + c_c^n) - Q_{cd} c_b^n) m_c^{n+1} + P_{cs}(c_m^n + c_c^n), \tag{3.59}$$

$$(I + \tau P_{cs}\kappa_c(c_m^n + c_c^n) + \tau Q_{cd} c_b^n) m_c^{n+1} = (m_c^n + \tau P_{cs}(c_m^n + c_c^n)). \tag{3.60}$$

3.4.6 Bone matrix density

Again the backward Euler scheme is used here:

$$\begin{aligned} \frac{\partial m_b}{\partial t} &= P_{bs}(1-\kappa_b m_b)c_b \\ &= P_{bs}c_b - P_{bs}\kappa_b c_b m_b, \end{aligned} \tag{3.61}$$

$$\frac{m_b^{n+1}-m_b^n}{\tau} = P_{bs}c_b^n - P_{bs}\kappa_b c_b^n m_b^{n+1}, \tag{3.62}$$

$$(I+\tau P_{bs}\kappa_b c_b^n)m_b^{n+1} = m_b^n + \tau P_{bs}c_b^n. \tag{3.63}$$

3.4.7 Cartilage growth factor concentration

The differential equations for the growth factors contain derivatives in space, so here the Finite Volume Method will be applied again. The equation was

$$\frac{\partial g_c}{\partial t} = \frac{\partial}{\partial x}(D_{gc}\frac{\partial g_c}{\partial x}) + E_{gc}c_c - d_{gc}g_c. \tag{3.64}$$

Using Finite Volume Method leads to

$$\begin{aligned} \int_{x_{j-1/2}}^{x_{j+1/2}} \frac{\partial g_c}{\partial t}dx &= \int_{x_{j-1/2}}^{x_{j+1/2}} \frac{\partial}{\partial x}\left(D_{gc}\frac{\partial g_c}{\partial x}\right)dx \\ &\quad + \int_{x_{j-1/2}}^{x_{j+1/2}} E_{gc}c_c dx - \int_{x_{j-1/2}}^{x_{j+1/2}} d_{gc}g_c dx, \end{aligned} \tag{3.65}$$

$$\begin{aligned} \int_{x_{j-1/2}}^{x_{j+1/2}} \frac{\partial g_c}{\partial t}dx &= \left[D_{gc}\frac{\partial g_c}{\partial x}\right]_{x_{j-1/2}}^{x_{j+1/2}} \\ &\quad + \int_{x_{j-1/2}}^{x_{j+1/2}} E_{gc}c_c dx - \int_{x_{j-1/2}}^{x_{j+1/2}} d_{gc}g_c dx. \end{aligned} \tag{3.66}$$

Integrate all terms:

$$\begin{aligned} \frac{\partial g_{c(j)}}{\partial t}h &= D_{gc(j+1/2)}\frac{g_{c(j+1)}-g_{c(j)}}{h} - D_{gc(j-1/2)}\frac{g_{c(j)}-g_{c(j-1)}}{h} \\ &\quad + E_{gc(j)}c_{c(j)}h - d_{gc(j)}g_{c(j)}h, \end{aligned} \tag{3.67}$$

and dividing by h

$$\begin{aligned} \frac{\partial g_{c(j)}}{\partial t} &= D_{gc(j+1/2)}\frac{g_{c(j+1)}-g_{c(j)}}{h^2} - D_{gc(j-1/2)}\frac{g_{c(j)}-g_{c(j-1)}}{h^2} \\ &\quad + E_{gc(j)}c_{c(j)} - d_{gc(j)}g_{c(j)}. \end{aligned} \tag{3.68}$$

Since D_{gc} and d_{gc} are constant

$$\frac{\partial g_{c(j)}}{\partial t} = D_{gc}\frac{g_{c(j+1)}-2g_{c(j)}+g_{c(j-1)}}{h^2} + E_{gc(j)}c_{c(j)} - d_{gc}g_{c(j)}, \tag{3.69}$$

so the vector differential equation becomes

$$\frac{\partial \underline{g}_c}{\partial t} = Z_{gc}\underline{g}_c + E_{gc}\underline{c}_c, \tag{3.70}$$

where the rows of Z_{gc} are given by

$$Z_{gc} = \left[\begin{array}{ccc} \frac{D_{gc}}{h^2} & -2\frac{D_{gc}}{h^2} - d_{gc} & \frac{D_{gc}}{h^2} \end{array} \right].$$

Applying the semi-implicit method and losing the underlines gives

$$\frac{g_c^{n+1} - g_c^n}{\tau} = Z_{gc}^n g_c^{n+1} + E_{gc}c_c^n \tag{3.71}$$

and finally

$$(I - \tau Z_{gc}^n)g_c^{n+1} = g_c^n + \tau E_{gc}c_c^n. \tag{3.72}$$

3.4.8 Bone growth factor concentration

The equation for g_b is the same as the one for g_c with changing the subscript c to subscript b, which leaves

$$(I - \tau Z_{gb}^n)g_b^{n+1} = g_b^n + \tau E_{gb}c_b^n, \tag{3.73}$$

where the rows of Z_{gb} are represented by

$$Z_{gb} = \left[\begin{array}{ccc} \frac{D_{gb}}{h^2} & -2\frac{D_{gb}}{h^2} - d_{gb} & \frac{D_{gb}}{h^2} \end{array} \right].$$

3.5 Model of Prendergast in 2D

In 2D only the discretisation for the equations for the cellular mesenchymal cell density and the fibrous cellular density have to be extended. The three-point method and the central scheme is used for discretisation in space and the backward Euler scheme for discretisation in time.

3.5.1 Mesenchymal cellular density

$$\begin{aligned} \frac{\partial c_m}{\partial t} = {} & D_m\nabla^2 c_m + P_m(1 - c_{tot})c_m - F_f(1 - c_f)c_m \\ & -F_c(1 - c_c)c_m - F_b(1 - c_b)c_m, \end{aligned} \tag{3.74}$$

$$\begin{aligned} \frac{\partial c_f}{\partial t} = {} & D_f\nabla^2 c_f + P_f(1 - c_{tot})c_f + F_f(1 - c_f)c_m - F_c(1 - c_c)c_f \\ & -F_b(1 - c_b)c_f. \end{aligned} \tag{3.75}$$

Discretising gives:

$$\begin{aligned}\frac{\partial c_m}{\partial t} &= D_m\nabla^2 c_m + P_m(1-c_c-c_f-c_b)c_m - P_m c_m^2 \\ &\quad -F_f(1-c_f)c_m - F_c(1-c_c)c_m - F_b(1-c_b)c_m\end{aligned} \tag{3.76}$$

$$\begin{aligned}\frac{\partial c_{m(i,j)}}{\partial t} &= D_{m(i,j)}\frac{c_{m(i-1,j)} - 2c_{m(i,j)} + c_{m(i+1,j)}}{h^2} \\ &\quad +D_{m(i,j)}\frac{c_{m(i,j-1)} - 2c_{m(i,j)} + c_{m(i,j+1)}}{h^2} \\ &\quad +P_{m(i,j)}(1-c_{c(i,j)}-c_{f(i,j)}-c_{b(i,j)})c_{m(i,j)} - P_{m(i,j)}c_{m(i,j)}^2 \\ &\quad -F_f(1-c_{f(i,j)})c_{m(i,j)} - F_c(1-c_{c(i,j)})c_{m(i,j)} - F_b(1-c_{b(i,j)})c_{m(i,j)} \\ &= (\frac{D_{m(i,j)}}{h^2})(c_{m(i-1),j} + c_{m(i+1),j} + c_{m(i,j-1)} + c_{m(i,j+1)}) \\ &\quad +(\frac{-4D_{m(i,j)}}{h^2} + P_{m(i,j)}(1-c_{c(i,j)}-c_{f(i,j)}-c_{b(i,j)}) - F_f(1-c_{f(i,j)}) \\ &\quad -F_c(1-c_{c(i,j)}) - F_b(1-c_{b(i,j)}))c_{m(i,j)}.\end{aligned} \tag{3.77}$$

So at the end it becomes a time-dependent vector-differential equation:

$$\frac{\partial \underline{c}_m}{\partial t} = Z_{cm}\underline{c}_m - P_m\underline{c}_m^2 + \underline{f}_m, \tag{3.78}$$

where the rows of Z_{cm} are represented by

$$\begin{bmatrix} & \frac{D_m}{h^2} & \\ \frac{D_m}{h^2} & \frac{-4D_m}{h^2} + P_m(1-c_c-c_f-c_b) - F_f(1-c_f) - F_c(1-c_c) - F_b(1-c_b) & \frac{D_m}{h^2} \\ & \frac{D_m}{h^2} & \end{bmatrix}$$

and

$$P_m = P_{m0}(1-m_c-m_b), \qquad D_m = D_{m0}(1-m_c-m_b). \tag{3.79}$$

The $N_x(N_x+1) \times N_x(N_x+1)$ matrix Z_{cm} has the form:

$$\begin{bmatrix}
B & 2A & & & & A & & & & & & & & & \\
A & \ddots & A & & & & \ddots & & & & & & & & \\
 & \ddots & \ddots & \ddots & & & & \ddots & & & & & & & \\
 & & A & \ddots & A & & & & \ddots & & & & & & \\
 & & & 2A & B & & & & & A & & & & & \\
A & & & & & B & 2A & & & & A & & & & \\
 & \ddots & & & & A & \ddots & A & & & & \ddots & & & \\
 & & \ddots & & & & \ddots & \ddots & \ddots & & & & \ddots & & \\
 & & & \ddots & & & & A & \ddots & A & & & & \ddots & \\
 & & & & A & & & & 2A & B & & & & & A \\
 & & & & & 2A & & & & & B & 2A & & & \\
 & & & & & & \ddots & & & & A & \ddots & A & & \\
 & & & & & & & \ddots & & & & \ddots & \ddots & \ddots & \\
 & & & & & & & & \ddots & & & & A & \ddots & A \\
 & & & & & & & & & 2A & & & & 2A & B
\end{bmatrix},$$

where

$$A = \frac{D_m}{h^2}$$

and

$$B = \frac{-4D_m}{h^2} + P_m(1 - c_c - c_f - c_b) - F_f(1 - c_f) - F_c(1 - c_c) - F_b(1 - c_b),$$

both dependent of the spatial coordinates (i, j). The 2's result from the Neumann boundary conditions.

The vectors $\underline{c}_m$ and $\underline{f}_m$ are represented by:

$$\underline{c}_m = \begin{bmatrix}
c_{m(0,1)} \\
c_{m(1,1)} \\
\vdots \\
c_{m(N_x,1)} \\
c_{m(0,2)} \\
c_{m(1,2)} \\
\vdots \\
c_{m(N_x,2)} \\
\vdots \\
c_{m(0,N_x)} \\
\vdots \\
c_{m(N_x,N_x)}
\end{bmatrix},$$

$$\underline{f}_m = \begin{bmatrix} Ac_{max} \\ \vdots \\ Ac_{max} \\ 0 \\ \\ \vdots \\ \\ 0 \end{bmatrix},$$

where the first entries of the vector f_m follow from the Dirichlet-boundary condition given on the periosteum.

For the discretisation in time the semi-implicit method is used, because of the non-linear term in the equation. It follows (for simplicity the underlining is left behind):

$$\frac{c_m^{n+1} - c_m^n}{\tau} = Z_{cm}^n c_m^{n+1} - P_m^n c_m^n c_m^{n+1} + f_m^n \tag{3.80}$$

Collecting terms gives:

$$c_m^{n+1} = c_m^n + \tau(Z_{cm}^n c_m^{n+1} - P_m^n c_m^n c_m^{n+1} + f_m^n) \tag{3.81}$$

and finally

$$c_m^{n+1} = (I - \tau(Z_{cm}^n - P_m^n c_m^n))^{-1}(c_m^n + \tau f_m^n) \tag{3.82}$$

3.5.2 Fibrous cellular density

For the fibrous cellular density the same procedure will be followed. Now all the boundaries have Neumann boundary conditions.

This results in a $(N_x+1)^2 \times (N_x+1)^2$ matrix Z_{cf}:

$$\begin{bmatrix}
B & 2A & & & & 2A & & & & & & & & & & \\
A & \ddots & A & & & & \ddots & & & & & & & & & \\
 & \ddots & \ddots & \ddots & & & & \ddots & & & & & & & & \\
 & & A & \ddots & A & & & \ddots & & & & & & & & \\
 & & & 2A & B & & & & & 2A & & & & & & \\
A & & & & & B & 2A & & & & A & & & & & \\
 & \ddots & & & & A & \ddots & A & & & & \ddots & & & & \\
 & & \ddots & & & & \ddots & \ddots & \ddots & & & & \ddots & & & \\
 & & & \ddots & & & & A & \ddots & A & & & & \ddots & & \\
 & & & & A & & & & 2A & B & & & & & A & \\
 & & & & & 2A & & & & & B & 2A & & & & \\
 & & & & & & \ddots & & & & A & \ddots & A & & & \\
 & & & & & & & \ddots & & & & \ddots & \ddots & \ddots & & \\
 & & & & & & & & \ddots & & & & A & \ddots & A & \\
 & & & & & & & & & 2A & & & & 2A & B
\end{bmatrix},$$

where

$$A = \frac{D_f}{h^2}$$

and

$$B = \frac{-4D_f}{h^2} + P_f(1-c_c-c_f-c_b) + F_f(1-c_f) - F_c(1-c_c) - F_b(1-c_b),$$

both depending on the spatial coordinates (i,j). Again the 2's result from the Neumann boundary conditions.

The vectors $\underline{c}_f$ and $\underline{f}_f$ are given by

$$\underline{c}_f = \begin{bmatrix}
c_{f(0,0)} \\ c_{f(1,0)} \\ \vdots \\ c_{f(N_x,0)} \\ c_{f(0,1)} \\ c_{f(1,1)} \\ \vdots \\ c_{f(N_x,1)} \\ \vdots \\ c_{f(0,N_x)} \\ \vdots \\ c_{f(N_x,N_x)}
\end{bmatrix} \text{ and } \underline{f}_f = \begin{bmatrix} 0 \\ 0 \\ \\ \vdots \\ \\ 0 \end{bmatrix}.$$

Chapter 4

Numerical Results

Before running the model due to Prendergast to simulate the bone-ingrowth process in 1D, the following values are chosen for the non-dimensionalized parameters:
$D_{m0} = 0.3456$, $D_{f0} = 0.1152$, $P_{b0} = 0.5$, $P_{c0} = 0.75$, $P_{m0} = 1.2$, $P_{f0} = 0.1$, $F_f = 0.01$, $F_c = 0.3$, $F_b = 0.15$, $Q_f = 0.06$, $Q_b = 0.1$, $Q_c = 0.2$, $D_b = Q_b$, $D_c = Q_c$, $c_{max} = 1$;
Time t is in days and the thickness of the prosthesis L, where the bone has to grow into, is chosen to be $10mm$.

4.1 Cellular and matrix densities

4.1.1 Results in 1D

Figure 4.1 represents the cellular densities of the four tissues after 3, 9, 30 and 60 days. The red line represents the mesenchymal cellular density, the blue line the fibrous cellular density. The cartilage and bone cellular densities are represented by respectively the cyan line and the green line.
The migration of the mesenchymal cells becomes clear in the plots for $t = 3$ and $t = 9$. At $t = 3$ the closer to the periosteum, the higher the density of mesenchymal cells and at $t = 9$ you can see a kind of wave pattern where the densities between $l = 4$ and $l = 8$ are higher then at $l = 3$.
As expected the level of chondrocytes is higher than the level of osteoblasts at the beginning of the process, but as time progresses the osteoblasts take over and keep growing, while the density of chondrocytes decreases.
The fibroblasts level stays very low during the whole process except very near the periosteum, where the density seems to grow a little.

Figure 4.2 represents the matrix densities of the different tissues. The level of fibrous tissue is very low and a closer look at the densities learns that its highest value is $m_f = 0.0039$. This value is reached after 15 days, whereafter it decreases again.
At time $t = 3$ already a little cartilage is formed and very little bone. At time

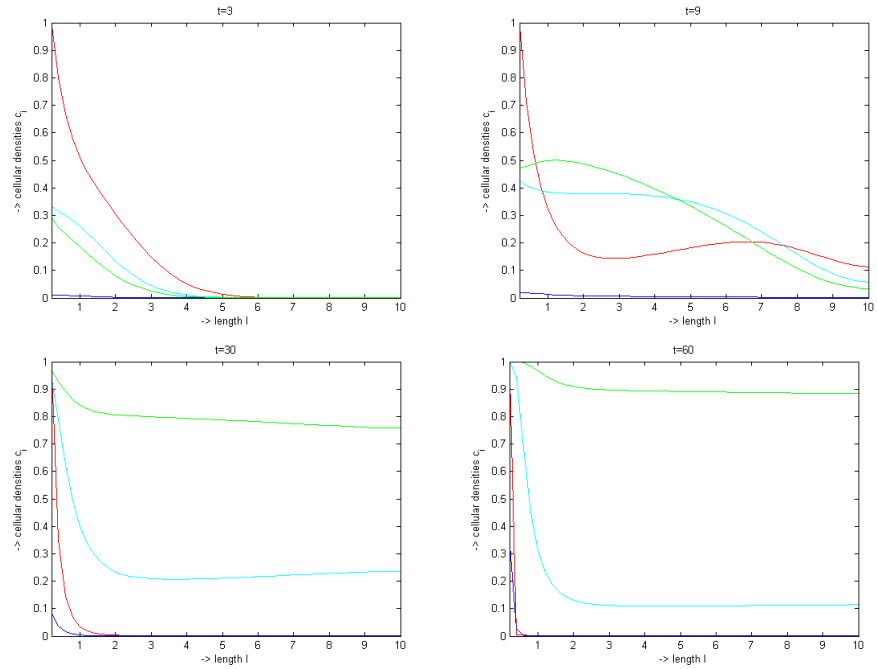

Figure 4.1: Cellular densities after 3, 9, 30 and 60 days. The red line represents the mesenchymal cells, the blue line the fibroblasts, chondrocytes are given in cyan and osteoblasts in green.

$t = 9$ the cartilage and bone tissues both increased, but there is still more cartilage than there is bone. Between $t = 9$ and $t = 30$ endochondral ossification takes place, because at $t = 30$ the cartilage level has decreased, while the bone tissue has grown. Around $t = 60$ almost all cartilage has disappeared and the whole tissue consist of bone.
It is interesting to find out when the endochondral ossification will take place. In figure 4.3 the matrix density at the periosteum is plotted against the time. It turns out that around $t = 15$ the endochondral ossification starts and the cartilage will be replaced by bone.

4.1.2 Results in 2D

Running the model in two dimensions gives comparable results. In figure 4.4 the density of the mesenchymal cells at $t = 9$ is shown and like in one dimension a wave pattern is observed. At the right the osteoblast density is plotted, which has the same pattern as in one dimension.
At the bottom the matrix densities of cartilage and bone are shown at $t = 15$, which is around the time that the endochondral ossification starts. At $t = 15$ the level of cartilage is still higher than the level of bone.

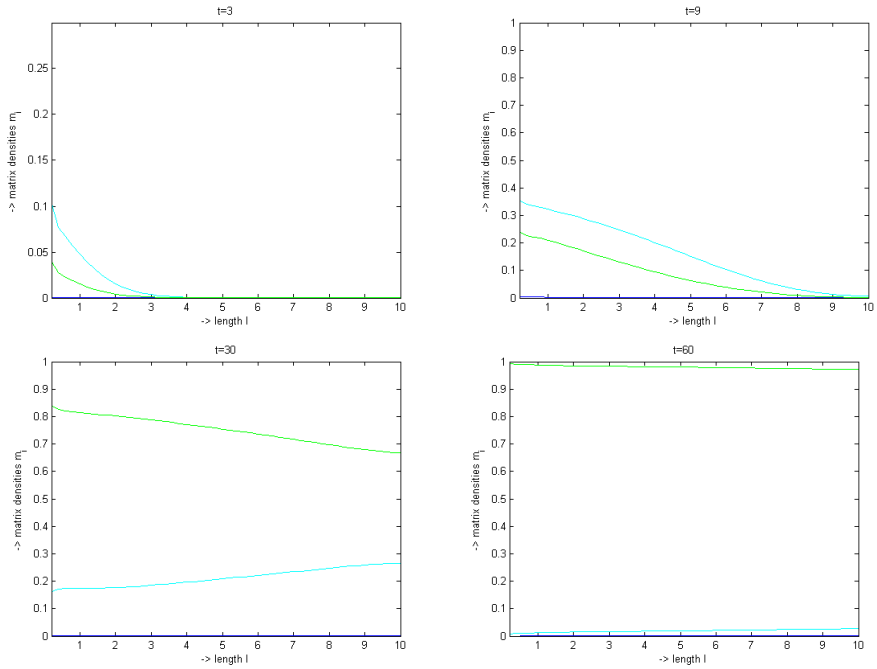

Figure 4.2: Matrix densities after 3, 9, 30 and 60 days. The blue line represents fibrous tissue, cartilage is given in cyan and bone in green.

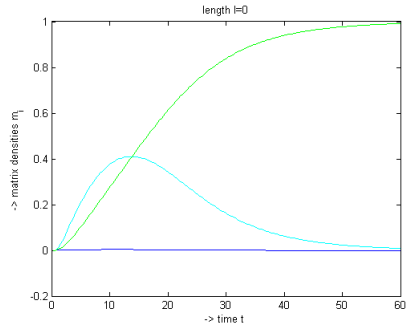

Figure 4.3: Matrix densities at the periosteum during time of healing. The blue line represents fibrous tissue, cartilage is given in cyan and bone in green.

4.2 Influence of parameters

It is assumed the bone is strong enough if the matrix density has reached level $m_b = 0.95$. Figure 4.5 shows the bone ingrowth in the whole length as a function of the time (in 1D). As mentioned the matrix density level is 0.95.
Simulation of the model gives that at $t = 42.3$ the bone growth starts near the periosteum and has grown into the whole length at time $t = 53.7$. It is interesting now to find out which parameters have the most influence on the rate of the bone ingrowth. To this purpose T is assumed to be the time the bone

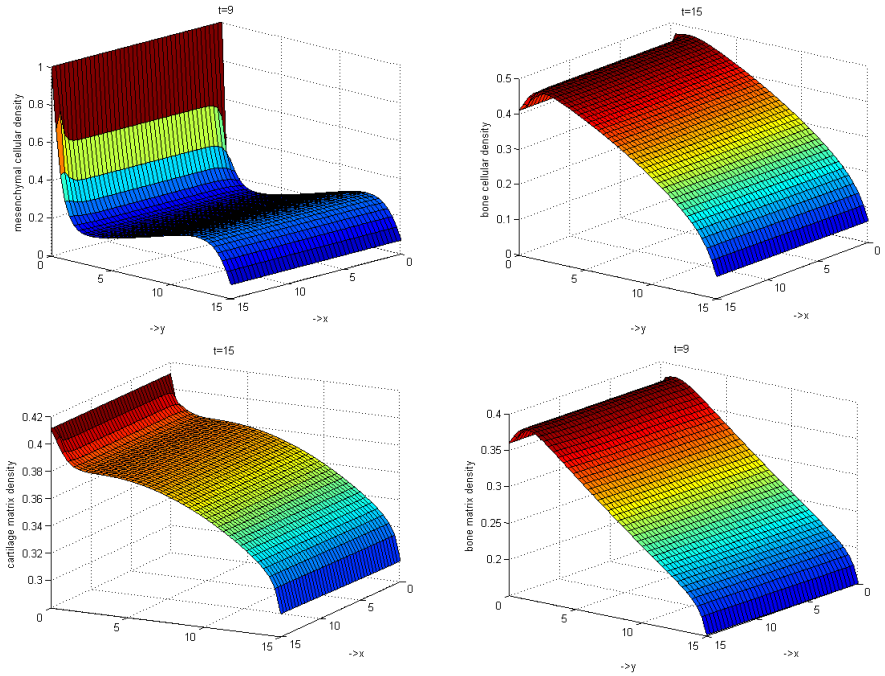

Figure 4.4: At the top left the mesenchymal cellular density is shown at $t = 9$. At the top right the density of the osteoblasts is given at $t = 9$. The plot at the bottom left represents the matrix density of cartilage at $t = 15$ and the plot at the bottom right the matrix density of bone at $t = 15$.

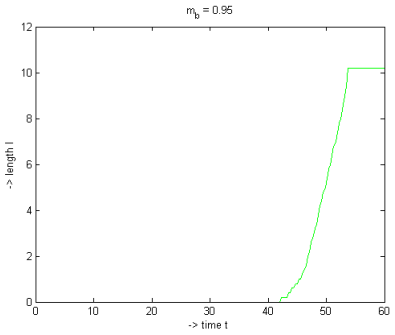

Figure 4.5: The bone ingrowth process starts at $t = 42.3$ and is finished at $t = 53.7$

is fully grown in. This T depends on the different parameters. The gradient vector of T around the given data for the parameters will be approximated and from this an estimate can be made for a measure of the sensitivity of the model to the different parameters. This will be done for the 1D model.

Using the central scheme and setting

$$T = T(D_{m0}, D_{f0}, P_{m0}, P_{f0}, P_{c0}, P_{b0}, Q_c, Q_b, F_f, F_c, F_b)$$

gives a gradient vector

$$\nabla T = \begin{bmatrix} \\ \partial T/\partial D_{m0} \\ \partial T/\partial D_{f0} \\ \partial T/\partial P_{m0} \\ \partial T/\partial P_{f0} \\ \partial T/\partial P_{c0} \\ \partial T/\partial P_{b0} \\ \partial T/\partial Q_c \\ \partial T/\partial Q_b \\ \partial T/\partial F_f \\ \partial T/\partial F_c \\ \partial T/\partial F_b \end{bmatrix} = \begin{bmatrix} -12 \\ 0 \\ -6.75 \\ 0 \\ 0 \\ -4.5 \\ 1.5 \\ -450 \\ 0 \\ 7.5 \\ -80.5 \end{bmatrix}$$

It is obvious that the parameters with the strongest influence are the bone production rate Q_b and the differentiation rate F_b. Also the mesenchymal diffusion coefficient D_{m0} and the proliferation rate of mesenchymal cells P_{m0} and osteoblasts P_{b0} have an impact, although much smaller. These parameters have the property that when their value increases, the bone growth will go faster.
The opposite holds for the proliferation rate P_{c0} and the differentiation rate F_c of the chondrocytes. When they increase the growth of the bone will go slower. Further the parameters relating to the fibroblasts and the fibrous tissue seem to have no effect at all.

Figure 4.6 shows the growth into the bone as a function of time for different values of Q_b and F_b. The red line represents the bone growth using the parameter values as used before. The green line shows the growth when the parameter values are increased and the black line when the value is decreased. It is clear Q_b has the greatest impact. When $Q_b = 0.05$ the growth has not even started at $t = 60$. Study learns it starts at $t = 75$ and at $t = 87$ the bone has fully grown in. For $Q_b = 1.5$ the bone ingrowth is finished considerably faster. For F_b the same can be concluded from the pictures, although the times of full ingrowth lie closer to each other.

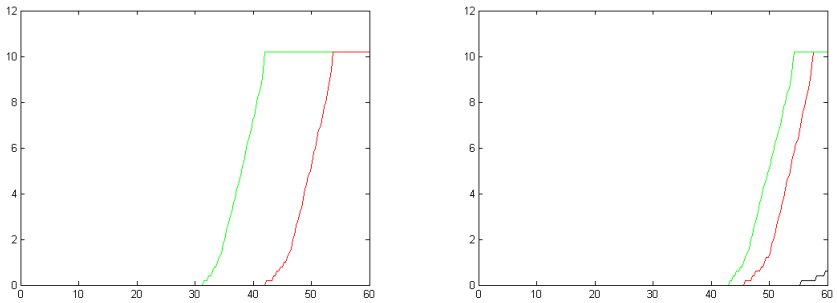

Figure 4.6: Values $Q_b = 0.05, 0.1, 0.15$ lead to full ingrowth at $T = 87, 53.5, 32.5$resp. and values $F_b = 0.05, 0.15, 0.25$ lead to full ingrowth at $T = 66.5, 53.5, 50.4$ resp.

Chapter 5

Conclusion

In this report the process of tissue differentiation during bone ingrowth into an shoulder prosthesis has been described. A comparison to the process of fracture healing has been made and two models to describe this process have been explained: the model due to Prendergast and the model due to Bailon-Plaza. A third model is briefly mentioned.

The model due to Prendergast in 1D has been implemented in MATLAB using the central scheme for discretisation in space and the (semi-implicit) Euler backward scheme for discretisation in time. After this the model is also simulated in 2D.
To determine the most influential parameters of the model the time T, where the bone has fully grown in, has been defined as a function of the parameters. The gradient vector of T has been approximated to find the most important parameters.

The results show that the values of the initial production rate of bone tissue Q_b and the differentiation rate to osteoblasts F_b have the biggest effect on the time where full bone ingrowth has been accomplished.
Also it has been shown that a change of parameters relating to fibrous tissue and the fibroblasts do not change the process of bone tissue production. This also holds for the initial proliferation rate of cartilage.
The production rate of cartilage tissue and the differentiation rate of chondrocytes have a inverse relation with the growth of bone. If their values increase, the process of bone growth will go slower.

Chapter 6

Future goals

In this paper it is assumed the mechanical stimuli is constant during the whole process, for the model of Prendergast. The next step is to add a tension field. This would be hypothetical, but should be taken as realistic as possible.
Then the model of Prendergast and the model of Bailon-Plaza will be compared. Since Bailon-Plaza models the growth factors and leaves out the fibroblasts and the mechanical stimuli, in comparison to the model of Prendergast, a combination of both models will be constructed.
Further, there exist a 3D implementation of the Prendergast model on an area of 1 mm^3, using Finite Elements. On this model, including the mechanics, a sensitivity analysis will be performed.

Bibliography

[1] Picture from: http://www.orthop.washington.edu/_Rainbow/Album/10357m9383d87a-fefa-4734-8e00-ede55900c0bc.gif

[2] Picture from: http://www.gla.ac.uk/ibls/fab/tutorial/generic/bone7.html

[3] http://wordnet.princeton.edu/perl/webwn?s=growth%20factor

[Adam, J. A. (1999)] A Simplified Model of Wound Healing (With Particular Reference tot he Critical Size Defect)*Mathematical and Computer Modelling 30, 23-32*

[Ament, Ch. and E. P. Hofer (2000)] A Fuzzy Logical Model of Fracture Healing. *Journal of Biomechanics 33*, 961-968

[Andreykiv, A (2006)] *Simulation of Bone Ingrowth.* Ph. D. thesis, TU Delft.

[Bailon-Plaza, A. and M. C. H Van der Meulen(2001)] A mathematical framework to study the effects of growth factors influences on fracture healing. *Journal of Theoretical Biology 212*, 191-209

[Burden, R. L. and J. D. Faires (2001)] *Numerical Analysis, 7th edition*, 277-280

[Wesseling, P. (2002)] *Elements of Computational Fluid Dynamics*, 22-28

List of Figures